# Weierstraß-Institut
## für Angewandte Analysis und Stochastik

im Forschungsverbund Berlin e.V.

Preprint ISSN 0946 – 8633


# Parallel simulation of high power semiconductor lasers


Mark Lichtner [1] and Martin Spreemann [2]



submitted: 23. May 2008



[1] Weierstrass Institute
for Applied Analysis
and Stochastics
Mohrenstraße 39
10117 Berlin, Germany
e-mail: lichtner@gmx.net

[2] Ferdinand-Braun-Institut
für Höchstfrequenztechnik
Gustav-Kirchhoff-Str. 4
12489 Berlin, Germany
e-mail: Martin.Spreemann@FBH-Berlin.de



No. 1326
Berlin 2008

2000 *Mathematics Subject Classification.* 65Y05, 37M05, 37L65, 35L45, 35Q60, 65M70, 65M06 .

*Key words and phrases.* parallel computation, numerical simulation of optoelectronic devices, laser dynamics, initial boundary value problem of hyperbolic type, comparison with experimental data.

Edited by
Weierstraß-Institut für Angewandte Analysis und Stochastik (WIAS)
Mohrenstraße 39
10117 Berlin
Germany

Fax: + 49 30 2044975
E-Mail: preprint@wias-berlin.de
World Wide Web: http://www.wias-berlin.de/

# Parallel simulation of high power semiconductor lasers

Mark Lichtner and Martin Spreemann

Weierstrass Institute for Applied Analysis and Stochastics
Mohrenstr. 39, 10117 Berlin, Germany
and
Ferdinand-Braun-Institut für Höchstfrequenztechnik
Gustav-Kirchhoff-Str. 4
12489 Berlin

**Abstract.** High power tapered semiconductor lasers are characterized by a huge amount of structural and geometrical design parameters and are subject to time-space instabilities like pulsations, self-focussing, filamentation and thermal lensing which yield restrictions to output power, beam quality and wavelength stability. Numerical simulations are an important tool for finding optimal design parameters, understanding the complicated dynamical behavior and for predicting new laser designs. We present fast dynamic high performance parallel simulation results, which are suitable for model calibration and parameter scanning of the long time dynamics in reasonable time, for a model based on traveling wave equations. Simulation results are compared to experimental data.

**Key words:** parallel computation, numerical simulation of optoelectronic devices, laser dynamics, initial boundary value problem of hyperbolic type, comparison with experimental data

MSC-class: 65Y05, 37M05, 37L65, 35L45, 35Q60, 65M70, 65M06

## 1 Introduction

Compact semiconductor lasers emitting single-frequency, diffraction limited beams at a continuous-wave (CW) optical power of several Watts are required for many applications including frequency conversion, free-space communications, and pumping of fiber lasers and amplifiers. Conventional narrow stripe or broad area semiconductor lasers do not meet these requirements, either due to limited output power or poor beam quality and wavelength stability. Such lasers are characterized by a huge amount of structural and geometrical design parameters and they are subject to time-space instabilities like pulsations, self-focussing, filamentation, thermal lensing which yield restrictions to output power, beam quality and wavelength stability. In particular an increase of width, length and pumping leads to several instabilities which can be seen experimentally and numerically in kinks in the powercurrent characteristics [1], beam-steering [2, 7],

and the appearance of higher order lateral modes in the lasing emission [3]. Possible reasons are carrierinduced index suppression, thermal lensing, and spatial hole burning [4].

In the past, numerous concepts to maintain a good beam quality and wavelength stability in the Watt range, have been proposed. One of the most promising devices is the monolithically integrated master-oscillator power-amplifier (MOPA), see figure 1, where either a distributed Bragg reflector (DBR) laser, or a distributed feedback (DFB) laser and a flared (or tapered) gain-region amplifier are combined on a single chip. CW optical powers of $1.1W$ or $2W$ [8, 9] have been achieved. During the last years, no further improvement towards higher output power has been reported. Recently, an improved MOPA, which emits a CW power of more than $10W$ at $977nm$ in a nearly diffraction limited beam and narrow spectral bandwidth of $40pm$, has been demonstrated by Ferdinand-Braun-Institut für Höchstfrequenztechnik in Berlin [6].

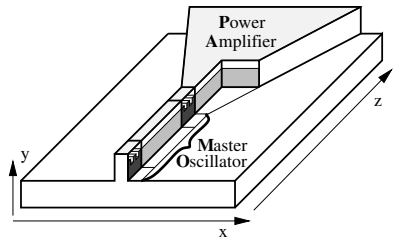


**Fig. 1.** layout of the MOPA device and system of coordinates used

For preparing technological processes to choose optimal parameters, to understand experimental data and for predicting new laser designs precise mathematical models for broad area semiconductor lasers are needed. As a next step suitable numerical algorithms have to be chosen and implemented. To adequately resolve the generation and propagation of photons for such laser devices one needs to use a spatial discretization which is of the order of the central wavelength of the laser (typically in the micrometer regime) - and use a time step of $\triangle t \sim c_0/(n_g \mu m) < 0.1ps$ ($c_0$ denotes speed of light and $n_g$ group velocity in the semiconductor medium). Due to a considerable length of several millimeters and width of several hundreds of micrometers for high power semiconductor lasers we obtain a large scale system of several million real spatial variables. Moreover, the carrier dynamics is in the order of $\sim 1ns$ being much slower than the photon equation. This implies relaxation times of several $ns$ which need to be simulated for different dynamical operating regimes. For the mentioned technological applications one is interested in multidimensional parameter studies or a bifurcation analysis [17], where different laser parameters like effective index steps, pumping levels, geometry of contacts or gratings are varied. For a reasonable resolution one dimensional parameter scan one needs to simulate dynamical

regimes involving more than 100 parameter steps and for a low resolution two dimensional parameter study pairs of several 1000 different parameters have to be considered. Considering a moderate simulation time of $2ns$ for each parameter a total simulation time of $2000ns$ or much more is required. Using a reasonable time discretization of $0.06ps$, which is the propagation time of the light in the semiconductor medium corresponding to a longitudinal discretization of $5\mu m$ - an adequate discretization to simulate lasers with a central frequency close to $1\mu m$ using a slowly varying envelope approach - , this means that $> 30$ million time iterations need to be performed. This can only be achieved in acceptable time by making use of parallel computation.

In this paper we present a mathematical model and a parallel simulation technique suitable for fast long time dynamical computation of high power broad area semiconductor lasers and show some parallel simulation results which we compare against experimental data.

## 2 Mathematical model

Using a slowly varying complex forward and backward traveling envelope $u^{\pm}$ (along the $z$ axis in figure 1) of the electric field, the effective refractive index method with a vertical (along the $y$ axis) single mode approximation, a paraxial approximation and a moving timeframe the $3d$ wave equation is reduced to a $2d$ wave equation in the $(x, z)$ plane [10, 12]. The resulting set of equations (1) consists of a hyperbolic system in the longitudinal $z$-dimension superposed with the Schrödinger operator along the lateral $x$-dimension describing diffraction of light. Equation (2) is a time domain description of a Lorentzian gain dispersion profile [16]. Equations (1) and (2) are nonlinearly coupled to the parabolic carrier equation (3) which can be derived from a standard carrier transport equation. The final system of equations has the following form:

$$\frac{1}{v_g}\partial_t u^{\pm} = \frac{-i}{2k_0\bar{n}}\partial_{xx}u^{\pm} + (\mp\partial_z - i\beta)\,u^{\pm} - i\kappa u^{\mp} - \frac{\overline{g}}{2}\left(u^{\pm} - p^{\pm}\right) \tag{1}$$

$$\partial_t p^{\pm} = \overline{\gamma}\left(u^{\pm} - p^{\pm}\right) + i\overline{\omega}p^{\pm} \tag{2}$$

$$\partial_t N = d_n\partial_{xx}N + I - R(N) - v_g\mathfrak{Re}\langle u, g(N,u)u - \overline{g}(u-p)\rangle_{\mathbb{C}^2} \tag{3}$$

with the reflecting boundary conditions

$$u^{+}(t,0,x) = r_0(x)u^{-}(t,0,x), \quad u^{-}(t,l,x) = r_l(x)u^{+}(t,l,x)$$

at the top ($z = l$) and bottom ($z = 0$) facet of the laser. Here $t \in \mathbb{R}$ denotes time, $z \in [0, l]$ longitudinal, $x \in \mathbb{R}$ lateral coordinate,

$$\beta = \delta_0(x,z) + \delta_n(x,z,N) + \delta_T(x,z,T) + i\frac{g(x,z,N,T) - \alpha(x,z)}{2}$$

is a propagation factor, where $g$ denotes peak gain, depending on the carrier inversion $N = N(t,x,z)$ within the active zone (averaged along the transversal

$y$ direction perpendicular to the layers), $\delta_0(x,z)$ is a built-in variation of the effective index independent on $N$ and the temperature $T$, $\delta_n$ and $\delta_T$ denote dependence of the index on $N$ and $T$, respectively. We use the following models for $g$ and $\delta_n$:

$$g = g(x,z,N,u) = g'(x,z)\frac{\ln\frac{N(t,x,z)}{N_{\mathrm{tr}}}}{1+\epsilon\|u\|^2},$$
$$\delta_n(x,z,N) = -\sqrt{n'(x,z)N(t,x,z)}.$$

Inhomogeneous electrical injection is denoted by $I = I(x,z)$, spontaneous recombination is given by

$$R(N) = A(x,z)N + B(x,z)N^2 + C(x,z)N^3$$

and the remaining expression in (3) corresponds to stimulated recombination. For the time being, temperature dependence is modeled via a linear dependence on the input current $I$:

$$\delta_T(x,z,T) = I(x,z)\cdot n'_T(x,z). \tag{4}$$

All coefficients with the exception of $k_0$, $v_g$ and $\bar{n}$ are spatially nonhomogeneous and discontinuous depending on the heterostructural laser geometry.

Well posedness (existence, unique, smooth dependence of solutions) of the model can be proved in a similar way as in [14] by using additional $L^\infty - L^1$ estimates for the Schrödinger semigroup along $x$.

## 3 Parallel simulation

We solve equations (1)-(3) using a split step method: the Schrödinger and elicptic operator are split off and solved using FFT. The splitting removes the coupling of the remaining hyperbolic system along the lateral $x$ dimension. It is solved for each $x$ by differencing along characteristics. For the stiff / fast dispersive polarization $p^\pm$ ($p^\pm$ operates in $fs$ regime in contrast to $u^\pm$ which is oscillating in the $ps$ regime) we use an exact exponentially weighted scheme using forward values for $u^\pm$. This ensures that in the limit for $\overline{\gamma}\to\infty$ the discrete solutions for $u^\pm$ and $p^\pm$ converge to each other, which is crucial for numerical stability. We have implemented the following parallel algorithm:

We split up the computation by decomposing the grid along the $z$ direction in uniform blocks, see figure 2. For each block we spawn separate processes which only operate on a single block and are distributed on several nodes of a cluster. Each process asynchronously transmits the boundary data (red) at junction grid points to its neighboring processes using non-blocked MPI sends in the beginning of each iteration (blue arrows in figure 2). For this the receiving process has to reserve ghost grid points in memory. Then the above split step method is executed for the interior grid points of the domain (black). FFT is performed by the fast FFTW library in multithreading mode [13]. We solve the decoupled set

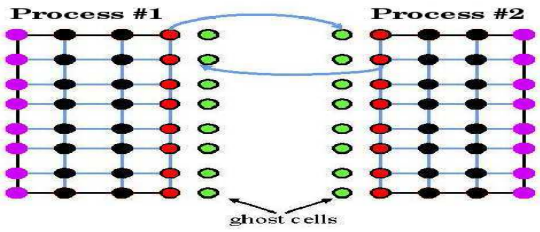


**Fig. 2.** decomposition of domain along $z$ direction in uniform blocks (for two processes)

of hyperbolic system parallel on multiple cores using multithreading with the POSIX threads library pthreads. The boundary grid points (red and pink) are solved after transmission of the boundary data at the end of each time step. For this we have synchronized threads using mutexes and conditions, so that only a single thread receives the boundary data using a blocked MPI receive while the others fall asleep. After all data have been received the threads are awakened and the boundary grid points are solved.

We have run simulations on a 32 node HP Blade server (HP CP3000BL 32xHP BL460c ) using the HPMPI library. Each node consists of two Intel Xeon Quad-Core (X5355). The nodes are interconnected via Infiniband 4xDDR (20 Gbit/s). For grid sizes of 320 000 and 640000, resulting in 2.88 or 5.66 million real spatial variables (corresponding to a $4mm$ or $8mm$ long and $250\mu m$ wide MOPA device with discretization $\triangle z = 5\mu m$, $\triangle x = 0.625\mu m$), and a parameter scan involving $1000ns$ simulation with time step $\triangle t = 0.061ps$ we report the following speedups:

| Nod. x Pro. x Thr. | laser length | grid | variables ($10^6$) | time |
|---|---|---|---|---|
| 1x4x2 | 4 mm | 800x400 | 2.88 | 285 h / 11.9 d |
| 1x4x4 | 4 mm | 800x400 | 2.88 | 290 h / 12 d |
| 4x4x2 | 4 mm | 800x400 | 2.88 | 75 h / 3.13 d |
| 4x4x4 | 4 mm | 800x400 | 2.88 | 73.8 h / 3.08 d |
| 9x4x2 | 4 mm | 800x400 | 2.88 | 37.5 h / 1.56 d |
| 9x4x4 | 4 mm | 800x400 | 2.88 | 36 h / 1.5 d |
| 1x4x4 | 8 mm | 1600x400 | 5.76 | 627 h / 26.1 d |
| 4x4x4 | 8 mm | 1600x400 | 5.76 | 147.8 h / 6.2 d |
| 9x4x4 | 8 mm | 1600x400 | 5.76 | 70 h / 2.92 d |
| 12x4x4 | 8 mm | 1600x400 | 5.76 | 57.2 h / 2.39 d |
| 18x4x4 | 8 mm | 1600x400 | 5.76 | 48.9 h / 2.04 d |

The first row of the table shows the number of nodes, processes per node and threads per process used. For example 9x4x2 means that the problem runs on 9x4=36 MPI processes which have been distributed on 9 nodes where each process uses 2 threads resulting in a total amount of 72 parallel threads. We found 4 processes with 16 threads per node to be optimal, except for the single noded case where there is a small drop down of performance probably due to context switching. A possible reason for this optimality is the dual-die dual-

core design of the Intel Quad Xeon design. For comparison, on a dual processor opteron 248 system (one core per processor) simulation time for a 4 mm laser is 1569 hours or 65.3 days.

Next we show some simulation and experimental results. Experimental results are taken from [15]. In figure 3 we see the simulated photon density distribution of the forward $|u^+|^2$ and backward field $|u^+|^2$ for a stationary CW state.

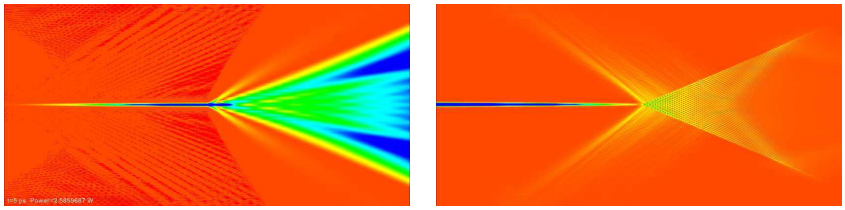

**Fig. 3.** Stable CW state: Photon density of forward (left) and backward field (right)

## 4 Simulation and experimental results

Power-current characteristics and optical spectra were measured for optoelectronic characterization of the MOPA devices. All measurements were taken under continuous wave conditions at 25 °C. After the assembling of a laser-diode the measurement of the power-current characteristics gives a general idea of its functionality. Quantum efficiency and threshold behavior can be extracted. The appearance of kinks points to instabilities in the laser operation.

The MOPA devices consist of a DFB laser as master oscillator (MO) and a flared (tapered) power amplifier (PA) which are separately driven. Therefore the output power is a function of two currents. The left part of Fig. 4 shows the measured optical power as a function of the PA current $I_{PA}$ for fixed MO currents $I_{MO}$ between 0.05A and 0.5A. For $I_{MO} > 0.4$ A the output power is in part independent of $I_{MO}$ and for 1 A $< I_{PA} <$ 4 A almost linear with $I_{PA}$. The slope is about 1 W/A and the maximum output power is 3.7 W. For $I_{MO} < 0.4$ A the MO current has strong influence on the maximum output power, the shape and the slope of the characteristic curve. The curve shows strong undulations of the output power with $I_{PA}$ as well as big drops of the output power at certain values of $I_{PA}$. This value of $I_{PA}$ increases with increasing $I_{MO}$. On the other hand the amplitude of the power undulations decrease with increasing $I_{MO}$. Apparently the PA gives some feedback to the MO and the effects on the MO are stronger at low MO currents. This assumption is approved by the simulation.

The right part of Fig. 4 shows the simulated power-current characteristics. In comparison with the experimental results it shows less optical powers which could be caused by the uncertainty of the model parameters. Furthermore the big drops of the output power can not be found in the simulation. Nevertheless

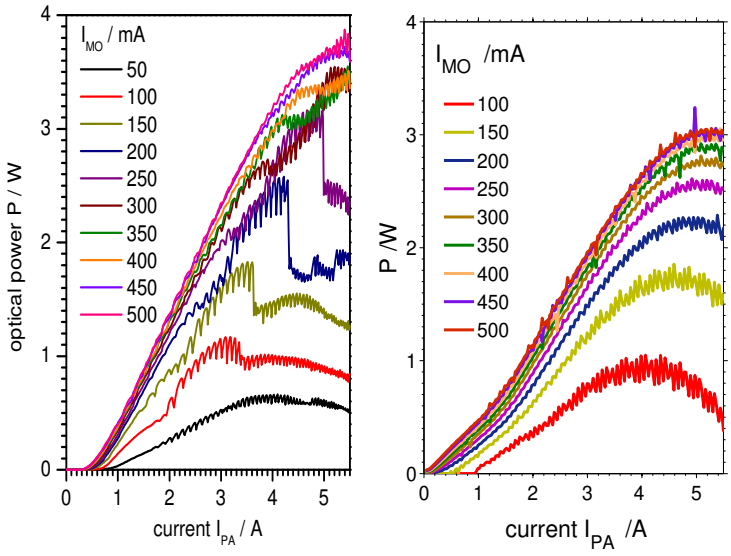


**Fig. 4.** Optical output power as a function of the input current to the PA. Parameter is the input current to the master oscillator. Left: experiment, right: simulation.

the other characteristics are reproduced. As in the experiment the amplitude of the power undulations depend on the MO current. When we decreased the front facette reflectivity in the model the undulations disappeared at all. This approves the assumption that feedback from the power amplifier into the master oscillator is the origin of the MOPAs instabilities.

The optical spectrum as a function of input current to the PA (Fig. 5) leads us to the underlying physical mechanism. The experimental results on the left side of Fig. 5 show a redshift of the peak wavelength and periodic change between single and multi-mode emission with increasing $I_{PA}$. Once per period a mode jump to a shorter wavelength mode occurs. During multi-mode emission the sidemodes have increased intensity but the total output power is decreased. This correlates with the undulations in the power-current characteristics. The simulation results on the right side of Fig. 5 reproduce the redshift, mode jumps and multi-mode behavior, although the current range with multi mode emission is much smaller than in experiment. Again the instabilities disappear when we reduce the front facet reflectivity in the model.

The MO DFB-Laser is designed for single longitudinal and lateral mode operation, but although the front facette of the MOPA is highly anti-reflection coated ($R < 10^{-4}$) the whole MOPA seems to work as a compound cavity. It has been reported that mode number, frequencies and losses are highly affected by feedback strength and phase in such cavities [5, 11].

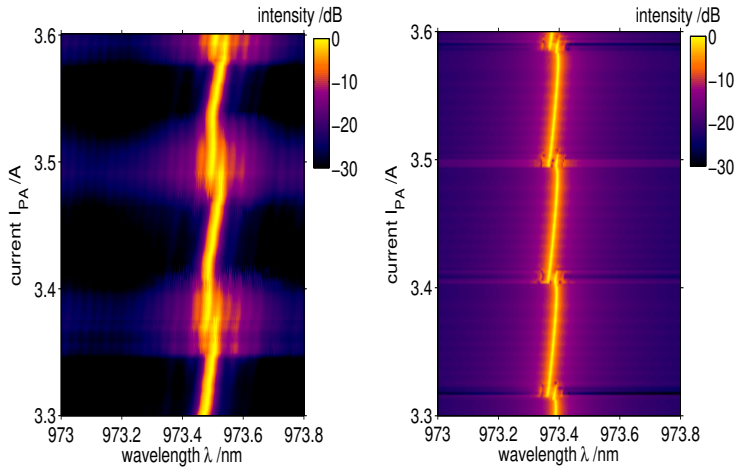


**Fig. 5.** Color-scale mapping of the optical spectrum as a function of the input current to the PA. The input current to the MO is $I_{\mathrm{MO}} = 0.35$ A. Left: experiment, right: simulation.

## 5 Summary/Conclusion

High power broad area semiconductor lasers are complicated devices which sensitively depend on a large set of different laser parameters. We have parallelized a suitable mathematical model which enables us to calibrate model parameters and perform parameter scans in reasonable time and have obtained first simulation results which are in satisfactory agreement with experiments. A more detailed comparison of simulation and experimental results will be subject to another paper. Simulations further show that besides other parameters the qualitative dynamical behavior depends sensitively on refractive index changes within the chip. In particular for broad area lasers, which produce a lot of heat, the impact of the temperature on the index is crucial. In our model the factor $n_T'$ in (4) has been fitted to experimental data. Simulations show that perturbations of $n_T'$ have a large impact on the number of mode jumps within a fixed interval of current pumpings. We expect to achieve better quantitative agreement by improving the temperature model for $\delta_T$. Since the temperature dynamics is several orders of magnitudes slower than the carrier dynamics the required computational power for a parameter study in reasonable time would be hitting the limit of todays available fastest clusters. Hence suitable simplified temperature models have to be developed.

*The authors would like to thank Hans Wenzel of FBH in Berlin for mathematical modeling and providing suitable laser parameters. Moreover we would like to thank Mindaugas Radziunas of Weierstrass Institute for sharing his experience regarding the numerics and dynamics of the traveling wave equations.*

## References


1. M. F. C. Schemmann, C. J. van der Poel, B. A. H. van Bakel, H. P. M. M. Ambrosius, A. Valster, J. A. M. van den Heijkant, and G. A. Acket: Kink power in weakly index guided semiconductor lasers, Appl. Phys. Lett., vol. 66, pp. 920922, 1995.
2. W. D. Herzog, B. B. Goldberg, and M. S. nl, Beam steering in narrow-stripe high-power 980-nm laser diodes, IEEE Photon. Technol. Lett., vol. 12, no. 12, pp. 16041606, Dec. 2000.
3. M. Achtenhagen, A. Hardy, and C. S. Harder, Lateral mode discrimination and self-stabilization in ridge waveguide laser diodes, IEEE Photon. Technol. Lett., vol. 18, no. 3, pp. 526528, Feb. 2006.
4. M. Achtenhagen, Transverse mode coupling in narrow-ridge waveguide laser diodes, Opt. Commun., vol. 266, pp. 171174, 2006.
5. S. Bauer and O. Brox and J. Kreissl and B. Sartorius and M. Radziunas and J. Sieber and H.-J. Wnsche and F. Henneberger, Nonlinear dynamics of semiconductor lasers with active optical feedback, Phys. Rev. E 69, 016206 (2004)
6. H. Wenzel, K. Paschke, O. Brox, F. Bugge, J. Fricke, A. Ginolas, A.Knauer, P. Ressel, G. Erbert, 10W continuous-wave monolithically integrated master-oscillator power-amplifier, Electronics Letters, Vol. 43, No. 3, 160-161 (2007).
7. H. Wenzel, F. Bugge, M. Dallmer, F. Dittmar, J. Fricke, K.H. Hasler, and G. Erbert, Fundamental-Lateral Mode Stabilized High-Power Ridge-Waveguide Lasers With a Low Beam Divergence, IEEE Photon. Techn. Lett., vol. 20, no. 3, pp. 214-216, Feb. 2008.
8. D. F. Welch, R. Parke, D. Mehuys, A. Hardy, R. Lang, S. OBrien, and S. Scifres, 1.1 W CW, diffraction-limited operation of a monolithically integrated ared-amplier master oscillator power amplier, Electron. Lett., vol. 28, no. 21, pp. 20112013, 1992.
9. R. Parke, D. Welch, A. Hardy, R. Lang, D. Mehuys, S. OBrien, K. Dzurko, and R. Scifres, 2.0 W CW, diffraction-limited operation of a monolithically integrated master oscillator power amplier, IEEE Photon. Technol. Lett., vol. 3, pp. 297300, 1993.
10. S. Balsamo, F. Sartori, and I. Montrosset, Dynamic Beam Propagation Method for Flared Semiconductor Power Ampliers, IEEE J. Sel. Top. Quantum Electron., VOL. 2, NO. 2, JUNE 1996
11. A.A Tager, K. Petermann, High-Frequency Oscillations and Self-Mode Locking in Short External-Cavity Laser Diodes, IEEE J. Quantum Electron., (1994), Vol.30, pp. 1553-1561
12. C. Z. Ning, R. A. Indik, and J. V. Moloney, Effective Bloch equations for semiconductor lasers and ampliers, IEEE J. Quantum Electron., vol. 33. pp. 15431550, 1997.
13. Matteo Frigo and Steven G. Johnson, The Design and Implementation of FFTW3, Proceedings of the IEEE 93 (2), 216231 (2005).
14. M. Lichtner, M. Radziunas, L. Recke: Well posedness, smooth dependence and center manifold reduction for a semilinear hyperbolic system from laser dynamics. Math. Meth. Appl. Sci., 30, 931960 (2007)
15. M. Spreemann, Nichtlineare Effekte in Halbleiterlasern mit monolithisch integriertem trapezförmigem optischen Verstärker, Diplomarbeit (Master thesis), Mathematisch-Naturwissenschaftliche Fakultät I, Humboldt-University Berlin, 25.6.2007

16. U. Bandelow and M. Radziunas and J. Sieber and M. Wolfrum, Impact of gain dispersion on the spatio-temporal dynamics of multisection lasers, IEEE J. Quantum Electron., (2001), Vol.37, no.2, pp. 183-188
17. M. Radziunas, Numerical bifurcation analysis of traveling wave model of multisection semiconductor lasers, Physica D, 213(1), pp. 98-112, 2006.